



Numerical assessment of indoor air quality in spaces in the United States designed with the ASHRAE 62.1–2019 Natural Ventilation Procedure

Troye Sas-Wright, Jordan D. Clark*

The Ohio State University College of Engineering, 221C Bolz Hall, 2036 Neil Avenue, Columbus, OH, 43210, USA



ARTICLE INFO

Keywords:

Natural ventilation
Fine particles
ASHRAE 62.1
Ventilative cooling
PM2.5

ABSTRACT

Natural ventilation is used to cool buildings and cut energy costs by inducing airflow through building openings without the use of mechanical ventilation and cooling systems. However, prior research has documented increased introduction of particles into indoor environments that are naturally ventilated, with associated health consequences. The recently updated ASHRAE Standard 62.1–2019: Ventilation for Acceptable Indoor Air Quality Natural Ventilation Procedure (NVP) prescribes opening sizes as a function of occupant density and geometry for use as a ventilation strategy, a change from the previous standard. The current work quantifies the indoor air quality impacts of implementing the Standard 62.1–2019 Natural Ventilation Procedure in the United States and compares it to the 62.1-specified ventilation rate procedure. This is done via coupled transient simulation of CONTAM 3.4 and EnergyPlus 9.1. Three pollutant classes were identified to represent a broad range of contaminants: outdoor-generated pollutants, pollutants generated indoors by humans, and pollutants generated indoors by the building itself. With boundary conditions from measured weather and outdoor pollutant data for 13 representative locations throughout the U.S., our modeling first found 41%–185% annual average increase in ventilation rates over its mechanical counterpart if the NVP is used across the geometries and occupant densities in the Standard. Due to elevated ventilation rates, the Natural Ventilation Procedure reduced building-generated and occupant-generated contaminant concentrations during occupied hours by an average of 17%–61% compared to the ventilation rate procedure. Outdoor-generated fine particles averaged 2.1–2.5 times the concentrations indoors when using the NVP as compared to mechanical ventilation with a MERV-8 filter and 7.8–10.4 times the concentration of a mechanical system with a MERV-13 filter. Both ventilation rates and concentrations were substantially climate-specific and somewhat window geometry-specific. We further showed that increased filtration is needed in many cases to keep up with increased effective NVP rates in the 2019 Standard if acceptable levels of indoor particles are to be achieved, and we offer suggestions for improving the Standard.

1. Introduction

Natural ventilation (NV) introduces unfiltered outdoor air into indoor environments to provide ventilation and cooling. NV is implemented mainly because of its benefits with respect to energy savings. NV provides fan energy savings as well as conditioning savings by bringing in cool outside air when weather is suitable, through building openings. Many studies have associated NV with energy savings, e.g. Refs. [1–3]. In addition to this, occupants are more tolerant of a wider range of temperatures in naturally ventilated buildings [4], allowing for wider setpoint bands and increased cost savings.

NV is driven by natural forces including wind pressures and the stack

effect—the movement of air due to differences in density. Since natural ventilation is a phenomenon that arises from naturally occurring and variable forces, rather than the predictable action of mechanical systems, resulting air quality in naturally ventilated buildings is less easily predicted than that in mechanically ventilated buildings (which itself is often challenging to predict). Furthermore, resulting indoor air quality, (IAQ), in NV buildings is a function of variables not under a designer's control, including weather and transient and/or mobile pollutant sources. However, methods exist for assessing the validity of the prescribed opening sizes and estimating their effect on resulting IAQ, which is the subject of the current work.

Prediction of ventilation rates through NV openings involves

* Corresponding author.

E-mail address: clark.1217@osu.edu (J.D. Clark).

accounting for the interaction between opening parameters, building variables and transient indoor and outdoor conditions. Multiple studies have characterized NV and its influencing forces [5–14]. Results of previous studies have shown the validity of the use of the orifice equation to predict natural ventilation rates [15], as well as the effects of opening geometry on NV rates [16]. Simulation software has been shown to reasonably model behavior of naturally ventilated zones, given appropriate boundary conditions and building parameters [17]. More specifically, the use of coupled simulation between CONTAM and EnergyPlus to analyze the relationship between ventilation and IAQ has been demonstrated repeatedly [17–21]. In the current work, such modeling will be used to analyze the ASHRAE/ANSI Standard 62.1–2019 NVP [22].

Multiple existing works examine natural ventilation's impact on IAQ. One variable affecting IAQ in all buildings [23], and especially NV buildings, is outdoor air quality. Unfiltered outdoor air is often introduced in large quantities into NV buildings [24–27]. In mechanically ventilated buildings, filtration within the air handler and management of outdoor air rates play an integral role in the reduction of fine particles in indoor environments, [3]. Fine particles are particles with aerodynamic diameters less than 2.5 μm and are often generated by combustion, industrial processes, and atmospheric chemistry processes. Several studies have shown that natural ventilation strategies introduce many particles of outdoor origin into indoor environments [28].

Because of the additional introduction of fine particles, multiple studies have noted the consequences of reduced IAQ in NV buildings. According to the World Health Organization, "Chronic exposure to particles contributes to the risk of developing cardiovascular and respiratory diseases, as well as of lung cancer" [29]. In most cases, control over the introduction of fine particulate matter into indoor environments is not available with NV and can result in increased exposure and consequent health effects. One study estimated that retrofitting 10% of California's office buildings for natural ventilation would result in 22,000–56,000 fewer workers experiencing sick building syndrome symptoms weekly [27]. This California study also estimated that a 10% retrofit would incur a net annual health-related cost of \$130–\$207 million caused by exposure to PM2.5 and ozone.

To minimize exposure to outdoor pollutants, hybrid systems designed for natural and mechanical ventilation based on outdoor air quality have been considered by researchers [30]. Hybrid mode ventilation simulations were developed to switch between mechanical and natural ventilation based on weather conditions and whether any of three outdoor pollutants exceeded the U.S. National Ambient Air Quality Standards. The study found a 5%–70% pollutant-related reduction in natural ventilation usage across locations in the U.S. when control based on ambient air quality was considered. Furthermore, the research identified fine particles as the "most significant issue in natural ventilation usage."

1.1. Background on changes to 62.1–2019 natural ventilation procedure

Given that there may be substantial health-related costs, and that adjusting the control of NV for ambient air quality can lead to large reductions in its use, ensuring proper standardization of NV designs is crucial. In an attempt to do so, the 2019 version of ASHRAE/ANSI Standard 62.1: Ventilation for Acceptable Indoor Air Quality includes updates to the Natural Ventilation Procedure (NVP) [22] in order to "provide a more accurate calculation methodology and also define the process for designing an engineered system. Natural ventilation now requires considering the quality of the outdoor air and interaction of the outdoor air with mechanically cooled spaces."

Opening sizes defined in the new prescriptive compliance path are specified in a more detailed manner than in previous versions of the standard, and a new definition of engineered natural ventilation systems is given. The major changes to the 2019 version of the prescriptive path include sizing prescriptions as a function of both ventilation intensity (a

Table 1

Reproduced Tables 6–5 and L-1 from standard 62.1–2019: Minimum openable areas: Single openings.

V _{bz} /A _z ≤ (IL/ s]/m ²)	V _{bz} /A _z ≤ (cfm/ ft ²)	Total Openable Areas in Zone as a Percentage of A _z			Commonly Encountered Typologies Bracket
		H _s / W _s ≤ 0.1	0.1 < H _s / W _s ≤ 1	H _s / W _s > 1	
1.0	0.2	4.0	2.9	2.5	Office, living room, main entry lobby
2.0	0.4	6.9	5.0	4.4	Reception area, general manufacturing, kitchen, lobby
3.0	0.8	9.5	6.9	6.0	Classroom, daycare
4.0	0.8	12.0	8.7	7.6	Restaurant dining room, places of religious worship
5.5	1.1	15.5	11.2	9.8	Auditorium, health club/ aerobics room, bar, gambling

function of occupant density), and opening geometry. Tables 6–5 from Standard 62.1–2019, referred to as Table 1 of the current work, is reproduced below to illustrate this change:

This is in contrast to previous versions of the Standard which prescribed only openings that had an area of 4% of the floor area to be ventilated, regardless of opening geometry or occupant density.

The 2019 NVP now specifies several opening geometries, five of which are suitable for buildings with normal 8–10 ft ceilings. These five geometries are shown in Fig. 1. Required opening dimensions are then specified as a function of geometry. This geometry-specific prescription of NV opening size is one of the more substantial changes to the 62.1 NVP from previous versions. In previous versions, prescriptive sizes were independent of geometry and only a function of floor area (4% of floor area) of the space to be ventilated. Giving geometry-specific prescription acknowledges the fact that stack-driven ventilation will be a function of opening geometry, but no annual calculations of resulting NV flows and resulting IAQ with these openings have yet been conducted, which motivates the current work.

The second substantial change in the 2019 NVP prescriptive path is that it prescribes ventilation rates according to space use type, where previously as mentioned a simple percentage of floor area was the only stipulation. The 2019 version acknowledges different needs of different space types by pegging NV opening sizes to required mechanical ventilation rates (see Table 1 of this work) for that space type. To do this, the NVP gives required opening sizes as a function of required mechanical ventilation rates (V_{bz} in Equation (1)), for each opening geometry. For example, spaces with greater occupant density such as lecture halls will have a greater ventilation intensity, V_{bz}/A_z , and therefore require greater sizes of NV openings.

The last prescription in the NVP of Standard 62.1–2019, unchanged from previous versions, is that in order to provide for adequate air distribution, the depth of the room in the direction normal to the natural ventilation opening must not exceed twice the height of the room in single-sided NV configurations.

Resulting IAQ in buildings designed with the 2019 NVP has not yet been studied, and the justification for its prescriptions is not explicit in the standard. An informative note on the 2019 changes states that "opening sizes have not been created to address thermal comfort", assumedly meaning their prescription is for indoor air quality (IAQ) purposes only. No further explanation or justification for the opening size prescriptions is given. Much of natural ventilation design is driven by thermal concerns and we suspect the standard prescriptions are as well, leaving resulting air quality to be assessed by others.

In order to fill this need, this work aims to:

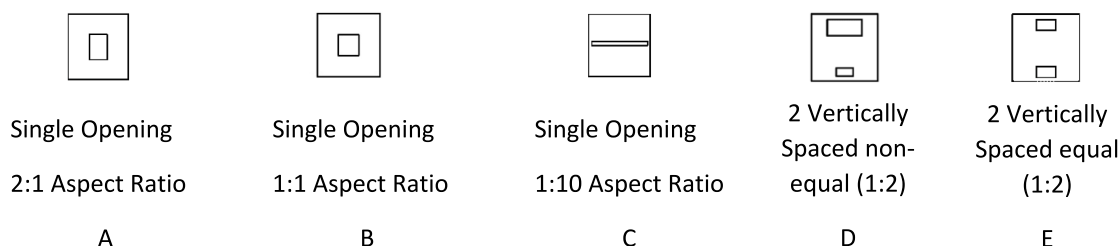


Fig. 1. Opening geometries.

1. Quantify ventilation rates expected with 62.1–2019 prescriptive path for NV
2. Estimate resulting IAQ in buildings designed with the NVP in terms of ventilation rates and resulting concentrations of particulate and gaseous pollutants
3. Understand significance for health effects in comparison to mechanically ventilated buildings designed with the ventilation rate procedure and the previous version of the standard

While many studies have quantified the impact of natural ventilation approaches on resulting indoor air quality, none have quantified the impact of the large changes to the 2019 Standard. For this reason, this study is a novel contribution to the literature in that it is the first to assess resulting IAQ in buildings ventilated using the 2019 and later NVP.

2. Methodology

2.1. Overall approach

Few buildings have yet been constructed that were designed with the ASHRAE 62.1–2019 NVP. Furthermore, measuring real-time ventilation rates in naturally ventilated buildings is exceedingly difficult and rarely done, as Persily et al. point out in their 2016 review of field measurements of ventilation [31]. The 2016 review only found two studies with measurement of NV rates and the generality and accuracy of both studies were in question.

For these reasons, we attempt to provide a robust estimate of IAQ in 62.1-designed NV buildings through an extensive modeling campaign. This campaign employs coupled simulation of CONTAM 3.4 and EnergyPlus 9.1 through a Functional Mock-up Interface (FMI) protocol previously developed [17,18]. We used EnergyPlus to model heat transfer across the building envelope, HVAC system operation and controls, and energy balance of interior spaces. We used CONTAM to model the air and contaminant mass balances including mechanical air flows and natural ventilation flows across exterior openings, contaminant generation, and contaminant transport. The geometry, aspect ratio, floor area and zone heights were specified in CONTAM to match the EnergyPlus model. At each time step, temperatures of the modeled space were sent from EnergyPlus to CONTAM, and airflow rates were sent from CONTAM to EnergyPlus. Temperatures affected stack-driven flow rates through natural ventilation openings, which then in turn affected the energy balance and resulting temperatures in the space. This communication was enabled by the FMI protocol, a standardized protocol for exchanging information among various simulation platforms (<https://fmi-standard.org/>). This process has been used successfully in several previous works including [19–21,67].

2.2. Ventilation strategies analyzed

Using this co-simulation framework, we analyzed two cases:

mechanical ventilation and mixed mode natural ventilation. We describe these in detail presently.

2.2.1. Case 1 - mechanical only

As a baseline, we first quantified resulting IAQ in spaces designed with the ASHRAE 62.1 Ventilation Rate Procedure (VRP) for mechanically ventilated spaces. The mechanical ventilation rate for each space was calculated with Equation (1), which is taken directly from the ASHRAE Standard 62.1–2019 VRP prescriptions.

$$V_{bz} = R_p \times P_z + R_a \times A_z \quad (1)$$

Where:

$$V_{bz} = \text{zone ventilation rate [L/s or cfm]}$$

$$A_z = \text{zone floor area [m}^2 \text{ or ft}^2\text{]}$$

$$P_z = \text{zone population [#]}$$

$$R_p = \text{outdoor airflow rate per person [L/s or cfm per person]}$$

$$R_a = \text{outdoor airflow rate required per unit area. [L/s/m}^2 \text{ or cfm/ft}^2\text{]}$$

The values of the parameters in Equation (1) are specified in Standard 62.1 and are a function of space type and occupant density. We varied these inputs systematically throughout the simulation campaign. Mechanical ventilation rates used as a baseline are given in Table 2. This spans several different ventilation intensities to give a representative sample against which to compare natural ventilation results.

2.2.2. Case 2 – mixed mode natural ventilation

The second case simulated assumes that the natural ventilation openings are operable or automatically controlled, and they open and close based on the suitability of outdoor conditions. During times when the temperature was between 60 °F and 80 °F and the relative humidity was less than 70%, the mechanical system was turned off and openings were used for ventilation according to best practice guidance [32]. When the temperature or humidity moves outside of these bounds, the mechanical system is turned on and the openings closed. Natural ventilation openings were sized according to the new NVP in ASHRAE Standard 62.1–2019 as described previously.

2.3. Building geometry and envelope

To define the buildings, we first used CONTAM 3.4 to specify building geometry, single-sided NV opening parameters, and contaminant sources. We created a one-story CONTAM building with one zone facing each of the four cardinal directions in order to capture differences in zone ventilation rates due to wind patterns. A ceiling height of nine feet was specified for most simulations, and then the remaining interior dimensions of each zone were designed to conform to the prescriptions in 62.1–2019. For most of our simulations, this resulted in an 18' deep room with 9' ceilings. Diagrams of the zone geometries analyzed are located in the Appendix in Figures A1 and A2. Envelope thermal

properties were defined based on the US DOE Commercial Reference Buildings: Small Office model. We assessed the sensitivity to this assumption by re-running the simulations with the envelope of a Mid-Rise Apartment reference model and that of a Classroom.

We sized all natural ventilation openings according to Standard 62.1–2019 (See Table 1 of this work). Opening widths were then fixed by floor area and aspect ratio for each zone. Detailed information on opening dimensions for each geometry are located in the appendix, Table A-1. For all simulations conducted in this work, we specified a discharge coefficient of 0.6 in keeping with the stated assumptions of Standard 62.1.

2.4. Schedules

Occupancy schedules were input based on the US DOE commercial reference building schedules in the form of a multiplier on peak occupancy [33] as shown in Fig. 2. The commercial reference buildings and schedules were specifically developed to model typical building construction and operation within the United States for EnergyPlus. The peak occupancy for each zone was calculated based on the ventilation intensity and underlying occupant densities designated for office spaces by the 62.1 Ventilation Rate Procedure. All simulations were conducted with assumed schedules of the Small Office Building reference building. However, we conducted sensitivity tests to assess the effects of specifying other schedules and include results of this test below in Section 3.

2.5. CONTAM-EnergyPlus integration

With a CONTAM model built, we generated an identical EnergyPlus model by exporting the building using the CONTAM3DExport tool [34, 35]. Thermal inputs were specified in the EnergyPlus model, which accounted for the energy balance within each zone. The maximum occupancy and occupancy schedule were subsequently used to generate internal heat gains due to people in the corresponding EnergyPlus model. Peak internal gains from lighting and equipment were assumed to be 10.76 W/m^2 , and 120 W per person was specified to align with the commercial reference values. All zones were considered to be well-mixed. Building constructions, lighting schedules, and miscellaneous equipment schedules were also sourced from the US DOE commercial reference building schedules for a Medium Office. As with occupancy schedules, we assessed the sensitivity of results to this assumption by varying these inputs to be those for mid-rise apartments and classrooms. Table A-2 and A-3 in the appendix provide U-Values for the climate specific constructions.

2.6. Locations modeled

Building constructions and weather were specified per climate zone with reference to the US DOE Reference Buildings. Thirteen climate zones across the United States were considered. These locations correspond to those analyzed in previous studies to represent the range of climates throughout the U.S [30]. We analyzed typical meteorological

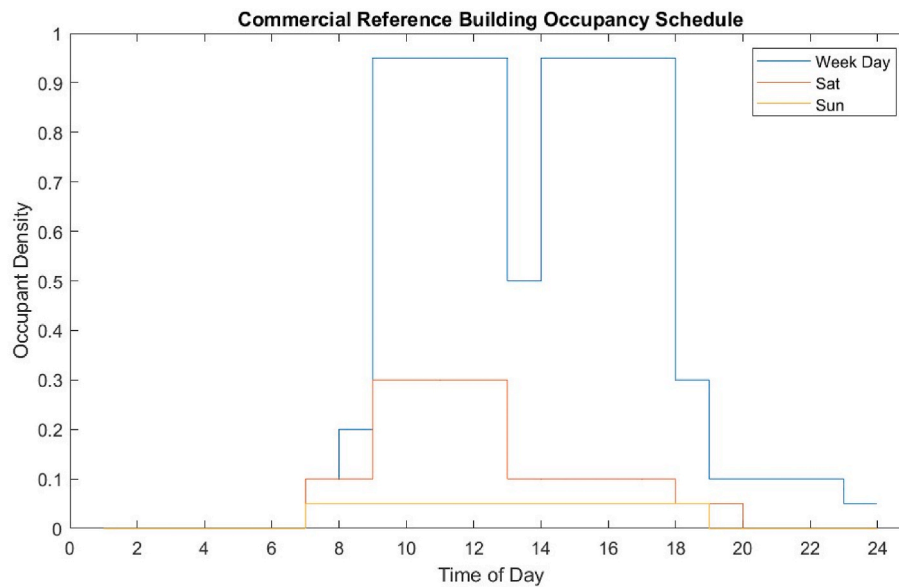


Fig. 2. DOE Relative Occupancy Schedule (Occupant Density of 1 implies peak occupancy).

Table 2

Occupancy & mechanical ventilation (baseline) rates.

Room size ft (m)	$V_{bz}/A_z \text{ cfm/ft}^2 (\text{L/s/m}^2)$	Peak Occupancy	$V_{bz} \text{ cfm (L/s)}$
10 × 18 (3.05 × 5.49)	0.2 (1)	5	36 (17)
10 × 18 (3.05 × 5.49)	0.4 (2)	12	72 (34)
10 × 18 (3.05 × 5.49)	0.6 (3)	19	108 (51)
10 × 18 (3.05 × 5.49)	0.8 (4)	27	144 (68)
10 × 18 (3.05 × 5.49)	1.1 (5.5)	37	198 (93)
28 × 18 (8.53 × 5.49)	0.2 (1)	14	101 (48)
28 × 18 (8.53 × 5.49)	0.4 (2)	34	202 (95)
28 × 18 (8.53 × 5.49)	0.6 (3)	54	302 (143)
28 × 18 (8.53 × 5.49)	0.8 (4)	75	403 (190)
28 × 18 (8.53 × 5.49)	1.1 (5.5)	105	554 (262)

Table 3
Location data.

City (abbreviation used)	Climate Zone	Avg PM _{2.5} Concentration (µg/m ³) (Data from 2018 to 2019)	Percentage of hours available for NV
Miami/Ft. Lauderdale (MIA)	1A	10.1	10%
Houston (HOU)	2A	21.8	11%
Phoenix (PHE)	2B	10.9	15%
Atlanta (ATL)	3A	16.6	12%
Los Angeles (LAA)	3B	19.9	25%
San Francisco (SFF)	3C	12.0	16%
Baltimore (BAL)	4A	9.1	10%
Albuquerque (ALB)	4B	9.7	15%
Seattle (SEA)	4C	7.5	12%
Chicago (CHI)	5A	11.7	10%
Denver (DEN)	5B	10.6	13%
Minneapolis (MIN)	6A	19.9	11%
Helena (HEL)	6B	17.4	12%

year (TMY) files and quantified the percentage of hours annually that had suitable conditions for NV. “Suitable” conditions were taken to be hours that had temperatures between 60 °F and 80 °F and relative humidity of less than 70% [32,36,37]. A summary of the locations and their average PM_{2.5} concentration from the time periods tested is summarized in Table 3. All locations were simulated for an entire year, with natural ventilation being employed when suitable, as described above in Section 2.2.

2.7. Pollutants modeled

We modeled three airborne pollutants, which in some cases were chosen to be representative of other pollutants of concern that may be encountered in indoor environments:

2.7.1. Fine particles generated outdoors

Numerous previous studies have pointed to particles of outdoor origin as being of most concern in naturally ventilated buildings. We defined outdoor concentrations of fine particles as specified in Section 2.10. We also specified other phenomena that are expected to contribute to the balance of particles in the space. These include internal sources, deposition, settling, and removal of particles by central filtration. However, in a 2017 literature review on airborne particles in indoor environments, Morawska et al. conclude that indoor sources of particles play a relatively small role on concentrations in office buildings compared to ambient particle concentrations [38]. Accordingly, the current work considers filtration, ventilation, and deposition to be the only contributors to the balance of fine particles in all simulations. We describe our assumptions for each of these presently.

2.7.1.1. Filtration. At the time of writing, MERV-8 filters are specified in Standard 62.1 as the minimum filter efficiency in mechanically ventilated buildings and MERV-11 filters for outdoor air intakes in buildings located in nonattainment areas for particles. However, it is understood that many buildings go beyond this, and many buildings installed MERV-13 filters during the Covid-19 pandemic. Much discussion is currently taking place in ASHRAE Standards Committees around specification of MERV-13 filters in both commercial and residential buildings. Knowing this, we specify a baseline of MERV-8 filtration in mechanical ventilation cases to filter all outdoor air. We also investigate resulting air quality if MERV-11 or MERV-13 filters are standardized in the future. The integrated fine particle removal efficiencies used in simulation were 24.8%, 37.7% and 67.6% for MERV-8, MERV-11, and MERV-13 filters respectively [39]. The simulation set also considers recirculation through the filter by fixing an outdoor air fraction of 20%

for all ventilation intensities (V_{bZ}/A_Z) in the standard.

2.7.1.2. Deposition. Deposition rates in the literature vary widely for fine particles, with estimates ranging from approximately 0.0918 h⁻¹ [40] to 1.63 h⁻¹ [41], with several works assuming intermediate values around 0.1–0.5 h⁻¹ [42–45]. Estimating deposition rates often requires some knowledge of the size distribution of particles, which is often not included in measured data and can vary based on the types of sources within an area. Estimating deposition rates specific to natural ventilation can lead to even more uncertainty due to the difficulty in measuring the ventilation rates themselves. With this in mind, a commonly used moderate fine particle deposition rate value of 0.2 h⁻¹ was assumed which was measured in the field [44] and used in a similar natural ventilation modeling campaign [30]. We also examine the sensitivity of the model results to this assumption in the Results Section.

2.7.2. Carbon dioxide generated indoors

Carbon dioxide was chosen to be representative of bioeffluents generated by humans. Source strengths of CO₂ are specified based on occupancy schedules, for metabolic activity characteristic of light office work. The maximum occupancy and occupancy schedules were used to apply a CO₂ source of 0.0051 L/s per person as reported for office and conferences spaces in commercial buildings [46].

2.7.3. Generic building-emitted gaseous contaminant

We modeled a generic gaseous pollutant to represent pollutants generated by the buildings and their furnishings. We do not specify the generic contaminant as we intend it to be representative of the host of gaseous pollutants generated indoors such as formaldehyde and other volatile organic compounds emitted from building materials and internal fixtures. The pollutant was emitted indoors at a constant rate throughout the simulation. This convention has been used for similar research several times previously and is the basis for the procedure outline in ASHRAE Standard 62.2–2019 Appendix C (2019b) [19,20,67], [21], [47], [48]. We specified a molecular weight for this pollutant identical to air, and present all results in normalized form, precluding the need for specifying source strengths or reporting any absolute concentrations. The only contributor to the balance of this generic pollutant was ventilation. No removal by filtration, deposition or reaction was included in the simulations in order to isolate the effect of ventilation, the subject of this work.

2.7.4. Reactive species not modeled

Reactive gases such as ozone were not modeled as necessary inputs are highly dependent on operating conditions and the contents of indoor environments, and thus any simulations made with simplifying assumptions would be of little value. Other works have examined the impact of natural ventilation on ozone concentrations [49,50]. Further experimental research is needed to understand the effect of the 2019 Standard prescriptions on reactive gas concentrations.

2.8. Boundary conditions

We applied weather boundary conditions such as ambient temperature and wind speed based on TMY3 files for each of the relevant locations. Weather boundary conditions were updated at each hour of the simulation. Outdoor air quality data was taken from EPA monitoring stations in the chosen areas between 2018 and 2019, depending on which year had a complete data set [51]. The TMY3 files are generated at hourly intervals, while EPA particle concentrations are reported at daily intervals. To resolve this, CONTAM interpolates all contaminant data down to the specified timestep. Outdoor concentrations of the generic gaseous pollutants were assumed to be zero to isolate the effect of ventilation on indoor-generated gaseous pollutants.

2.9. Model generation

Model geometries were formulated in CONTAM and exported into EnergyPlus as described in the previous sections. Next, CONTAM Parametric Analysis Utilities including ContamFactorial and EnergyPlus-CONTAM Co-Simulation Multiprocessing were used to create permutations of window geometries, filters, deposition rates, and ventilation supply rates and simulate results [52]. We flagged variables in the CONTAM project file and EnergyPlus idf file for perturbation, specified the sets of changes to make the variables, and used ContamFactorial to generate models for each permutation needed for the current work.

Next, the Co-Simulation Multiprocessing tool uses a list of EnergyPlus EPW weather files, idfs, and CONTAM projects to generate FMU files and run all of the permutations. The Co-Simulation tool leverages a Python-based multiprocessing package to run multiple simulations at once and generate EnergyPlus Results Files. The simulation process produced over 1500 simulation results that were then read and processed using the assessment techniques described in Section 2.8 of the current work.

2.10. Assessment techniques

To quantify the differences in resulting IAQ between the mechanical and mixed mode ventilation cases, metrics such as relative ventilation rates, relative concentrations, and relative exposure were used. Utilizing relative metrics allows for easy comparison and prevents the need for specification of highly uncertain parameters. It also negates some dependence on some of the inputs that were defined, such as occupancy schedules. The following descriptions summarize the calculations completed in this work. All metrics are integrated over the entire year.

2.10.1. Relative ventilation rate

Average relative ventilation rate reported in this work is given as the annual average during the occupied hours that utilize natural ventilation. Occupancy is considered because we are interested in the ventilation rates times when occupants are present and being exposed to possible pollutants in the ventilation air. The building is considered to be occupied when occupancy is more than 10%.

$$RV = \frac{\sum_{i=0}^t Occ_i * \frac{\dot{V}_{NVi}}{\dot{V}_{MVi}}}{\sum Occ_i} \quad (2)$$

Where:

RV = Average relative ventilation rate when natural ventilation is in use [–]

\dot{V}_{NVi} = Ventilation rate in the NV case [cfm or m^3/h]

\dot{V}_{MVi} = Ventilation rate in the MV case [cfm or m^3/h]

$$Occ = \begin{cases} 1; \text{ If building is occupied} \\ 0; \text{ Otherwise} \end{cases}$$

Using this metric, $RV = 1$ corresponds to equal ventilation rates between the natural and mechanical cases; $RV < 1$ denotes times when NV rates are less than MV rates, and vice versa.

2.10.2. Relative exposure

Exposure refers to the degree to which occupants are exposed to a pollutant of interest and thus includes a quantification of pollutant concentration. The exposure calculations specify occupant presence as a binary variable (present or not) as defined in Equations (2) and (3) above. However they consider the absolute concentration of the contaminant instead of relative concentration. For the case of CO_2 and the generic gaseous pollutant we report average relative exposure. Average relative exposure is calculated similarly to the relative ventilation rates:

$$RC = \frac{\sum_{i=0}^t Occ_i * \frac{C_{NVi}}{C_{MVi}}}{\sum Occ_i} \quad (Equation 3)$$

Where:

RC = Average relative concentration while natural ventilation is in use [–]

C_{NVi} = Concentration in the NV case [$\mu\text{g}/\text{m}^3$ or ppm].

C_{MVi} = Concentration in the MV case [$\mu\text{g}/\text{m}^3$ or ppm]

$$Occ = \begin{cases} 1; \text{ If building is occupied} \\ 0; \text{ Otherwise} \end{cases}$$

2.10.3. Exposure

We found it more informative to specify absolute exposure in the case of the fine particles in order to compare to published thresholds and assess health effects [53]. No such consensus thresholds exist for CO_2 and the generic pollutant. Unlike relative exposure, the exposure takes into account the particle concentration behavior over all occupied hours, instead of only comparing hours when NV is utilized. Equation (4) below describes the annual average exposure calculation.

$$E = \frac{\sum_{i=0}^t Occ_i * C_i}{\sum Occ_i} \quad (4)$$

Where:

E = Average exposure over all occupied hours [$\mu\text{g}/\text{m}^3$ or ppm].

C_i = building average concentration at each timestep [$\mu\text{g}/\text{m}^3$ or ppm]

$$Occ = \begin{cases} 1; \text{ If building is occupied} \\ 0; \text{ Otherwise} \end{cases}$$

2.11. Sensitivity analysis

To analyze the effects of highly variable or uncertain parameters within the model, a sensitivity analysis was performed with respect to space type and particle deposition rate. This analysis uses the San Francisco climate and particle data as a representative location to determine how sensitive our results are to changes in model parameters.

To capture the effects of using the NVP for design of different space types we modeled a primary school classroom and a dormitory room for comparison to the results from the office space type, keeping minimum filtration and all other parameters fixed. DOE reference building schedules and loads for bedrooms in mid-rise apartments and primary schools were used as inputs, as was done with the office space type [33]. In addition to loads and schedules, CO_2 breathing rates for bedrooms and primary schools with children older than 9 were used for the respective dorms and schools [46]. Information on peak load and CO_2 breathing rate assumptions can be found in appendix Table A-7.

As mentioned previously, particle deposition rate is a highly uncertain value. Values for this parameter integrated across size-resolved distributions for particles are usually considered to be less than 1 h^{-1} although some studies have suggested higher [41]. Since reported fine particle deposition rates are highly uncertain and range widely in the literature, another sensitivity analysis was performed on this parameter. The deposition rate varied between both the lowest and highest rates reported in the literature, $0.09\text{--}1.65 \text{ h}^{-1}$ as well as an intermediate rate, 0.5 h^{-1} for comparison to the chosen rate of 0.2 h^{-1} . The resulting relative particle concentrations were then compared.

3. Results and discussion

In this section we first give a verification of simulation performance and then present the results of the simulation campaign, as quantified by

Table 4
Reported I/O ratios for naturally ventilated buildings.

Reported PM2.5 I/O Range				
Source	Range Min	Range Max	Data Type	Notes
[3] Ben-David et al.	0.453	1.02	Simulated	MERV-8 Mixed mode strategy
[27] Dutton et al.	0.48	1.31	Measured	Office 2 (Mixed Mode Ventilation Strategy)
[61] Challoner & Gill	0.59	4.68	Measured	Office space during working hours
[62] Razali et al.	0.5	1.4	Measured	Naturally Ventilated Classrooms
[63] Dorizas et al.	1.02	4.97	Measured	Naturally Ventilated Classrooms

the relative metrics described in the previous section and organized according to the phenomenon of interest. Discussion of results and implications is given in Section 4.

3.1. Verification of simulation performance

As mentioned previously, vanishingly few field studies have measured ventilation rates in naturally ventilated buildings [31] and thus comparison of simulation results with field-measured rates is not feasible. Similarly, measured time series of particle concentrations in NV buildings are of little value if ventilation rates are not known. Instead, particle concentrations in naturally ventilated buildings are often quantified in terms of indoor/outdoor particle concentration ratios (I/O), averaged over multiple days. We currently review some of those measured I/O ratios and compare to the current work as a means of verifying simulation performance.

Martins et al. [24] provides a review of field studies measuring PM2.5 I/O ratio in commercial buildings, concluding that naturally ventilated buildings with low internal particle sources yield I/O ratios near one. This compares well with the results of the current study which show an I/O ratio around 1 in most cases for NV and MM cases with only MERV 8 filtration. Other researchers [54–60] provide other examples of studies measuring fine particles in naturally ventilated spaces for different building types, but either do not report I/O ratios or are conducted in less relevant space types. Using the assumption that particle I/O ratios are close to one during natural ventilation, [30] demonstrated the capability of their model by showing that fluctuations of indoor and outdoor pollutant concentrations closely followed each other

throughout their transient simulations.

Most relevant to the current study is likely a previous California study that measured I/O ratios for multiple office buildings located near Oakland, California utilizing various methods and combinations of natural and mechanical ventilation [27]. Particle measurements for Office 2 located in Oakland, identified an I/O ratio ranging from 0.48 to 1.31 during the day with a mixed mode ventilation setup. The current work's average simulated I/O ratio for nearby San Francisco was 0.87 in natural ventilation mode, falling within the field measurement range. It should be noted that while the current work does not include internal sources, it does include deposition. We also expect internal sources to be small in most commercial spaces without cooking sources.

Table 4 shows a selection of other relevant reported ranges for PM2.5 I/O ratios analyses for commercial spaces that are most similar to the current work. Again, results of the current work compare favorably with these ratios.

In addition to I/O ratios for particles, the aforementioned study [27] also reported measured ventilation rates ranging from 0.48 to 1.73 air exchanges per hour in the Oakland office. In the current study the simulated average air exchanges per hour (ACH) rates resulting from the ASHRAE 62.1-19 openings in mixed mode ventilation ranged from 1.9 to 12.7 per hour depending upon the design ventilation rate, V_{bz} , for San Francisco weather conditions. Simulated ventilation rates were notably higher than the measured values, presumably because it is unlikely that the window openings of this office space meet the standards specified in ASHRAE 62.1-19. Window sizes were not reported in this study.

3.2. Resulting ventilation rates

We presently examine the amount of outdoor air introduced into the spaces under different ventilation strategies, which may serve to explain resulting contaminant concentrations below. **Fig. 3** shows relative ventilation rates over the thirteen simulated locations for the 2:1 aspect ratio opening geometry (Geometry A). Occupant densities are designated by the amount of air required by the VRP in 62.1, per floor area (V_{bz}/A_z). A representative target ventilation intensity of 0.6 cfm/sqft was used in this figure. As expected, the locations yielded ventilation rates greater in the NV case than in the baseline MV case, with results varying between locations. Across all locations, occupant densities and geometries, the annual average natural ventilation rates were greater than the VRP ventilation rates. Annual average NV rates ranged 41%–185% greater than the VRP ventilation rates across the climates modeled. A summary of simulations run for climate and occupancy are

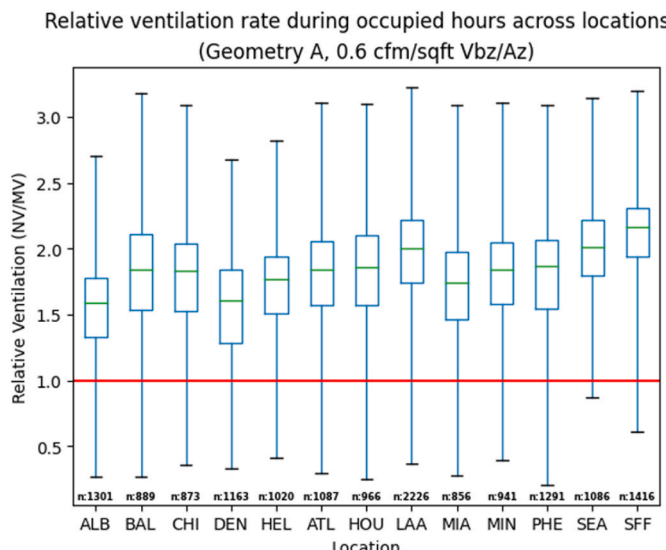


Fig. 3. Relative ventilation rates during occupied hours across locations.

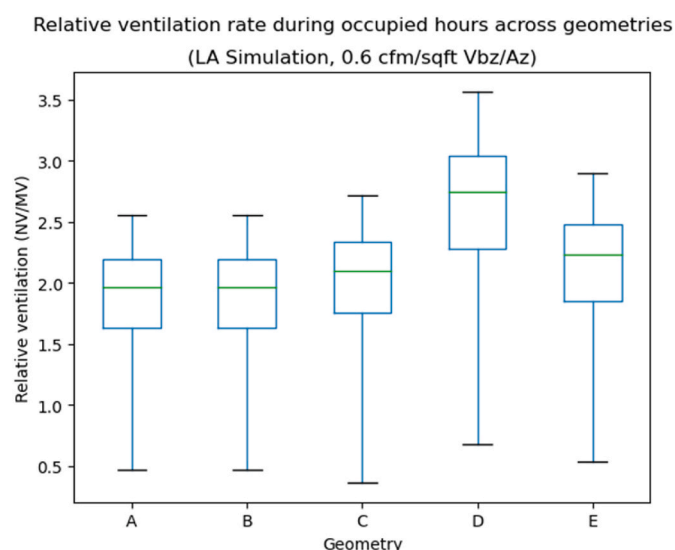


Fig. 4. Relative ventilation rate vs geometry (0.6 cfm/sqft Vbz/Az).

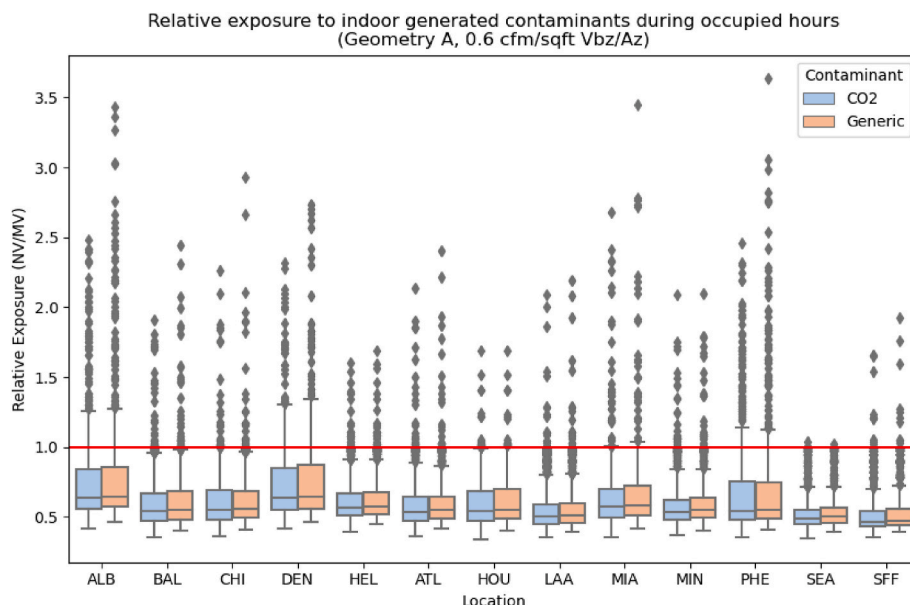


Fig. 5. Relative concentrations across location, (Geometry A, 0.5 cfm/sqft V_{bz}/A_z).

Table 5

Summary of annual relative concentrations across simulations.

Contaminant	Filter	mean	min	25%	50%	75%	max
fine particles	MERV8	2.39	2.10	2.32	2.42	2.46	2.52
	MERV11	3.52	3.00	3.42	3.59	3.66	3.74
	MERV13	9.61	7.80	9.26	9.83	10.11	10.37
CO ₂	n/a	0.57	0.39	0.51	0.56	0.62	0.79
Generic	n/a	0.58	0.40	0.52	0.58	0.64	0.83

included in Table A-4 and A-5 in the appendix.

3.2.1. Effect of geometry

We also investigated the effect of the opening geometries on resulting ventilation rates. Fig. 4 shows the relative ventilation rates across the five opening geometries specified in Fig. 1. All geometries tested yielded relative ventilation rates greater than one. The two vertically separated opening cases, (geometries D and E) resulted in greater ventilation rates than the others, with the disparately sized vertically separated case, (D) having the greatest ventilation rates. This suggests that even if climate weren't considered, changes could be made to the Standard to specify rates more uniformly across geometries. A summary of the simulation sets' relative ventilation rates grouped by geometry is provided in appendix Table A-6.

3.3. Indoor-generated pollutant concentrations

As expected, indoor generated pollutants were diluted more effectively while the ASHRAE 62.1 NV openings were in use since they provided overall greater ventilation rates. Fig. 5 summarizes the resulting concentrations of indoor-generated gaseous pollutants, given as boxplots of hourly relative concentrations for the various locations modeled for a representative geometry and occupant density. Note that for all locations both the median and inner quartiles for relative concentration were less than one. However, there are hours when the relative concentration was much greater than one because of low natural ventilation rates that sometimes arise from transient weather conditions. Due to the variable nature of natural ventilation, low windspeeds or small differences in indoor and outdoor temperatures lead to periods of elevated contaminant concentrations when compared to mechanically ventilated cases. In Fig. 5, the outliers, or hours that lie outside of

Table 6

Pre-2019 assumed occupant density based on Geometry.

Geometry	Pre-2019 Ventilation Intensity V_{bz}/A_z cfm/ft ² (L/s/m ²)
A	0.36 (1.8)
B	0.30 (1.5)
C	0.2 (1.0)
D	0.63 (3.2)
E	0.98 (5.0)

$1.5 \times$ the interquartile range, are plotted as points beyond the whiskers. Outliers included times when the NV concentrations are up to 3.5 times greater than those resulting from MV.

In all cases tested, behavior of the generic contaminant and CO₂ were not much different from each other. Although their source strengths temporally vary in different ways, the relative concentration metric only takes into account hours when occupants will be exposed to the gaseous contaminants and only compares their behavior under NV with respect to MV.

Relative concentrations for other geometries and occupant densities followed the same pattern. Distributions of relative concentrations roughly mirrored the inverse of the performance of the relative ventilation rates. Average relative concentrations for the indoor-generated gaseous contaminant showed a decrease from 17% to 61% when using NV versus MV. Table 5 shows the distribution of annual average relative concentrations across the various locations, occupant densities, and geometries tested for both the generic contaminant and CO₂. Small differences between the relative concentrations of the generic pollutant and CO₂ are explained by the differences in emission rates. As noted in the methods section, the generic pollutant is emitted at a constant rate, while CO₂ is emitted based on occupancy schedules.

3.4. Fine particles

In general, indoor fine particle concentrations followed outdoor concentrations when natural ventilation was employed. Fig. 6 shows the resulting annual average exposure to PM_{2.5} over the year for mechanical ventilation (MV) with MERV-8 filtration; MV with a MERV-11 filter; MV with a MERV-13 filter; and NV for the 13 representative locations modeled at a representative geometry and occupant density. Although occupancy density had a small effect on exposure via the size of the

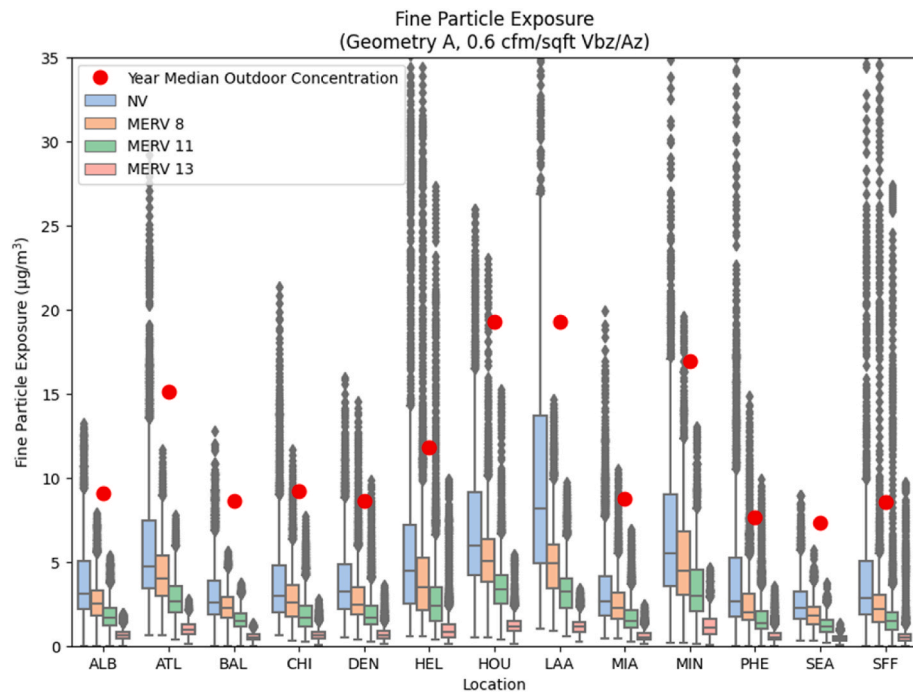


Fig. 6. Fine Particle Exposure by Location. Note: LAA is a non-attainment area with regard to PM2.5, and therefore neither the MERV8 case nor the natural ventilation case are compliant with Standard 62.1 as written.

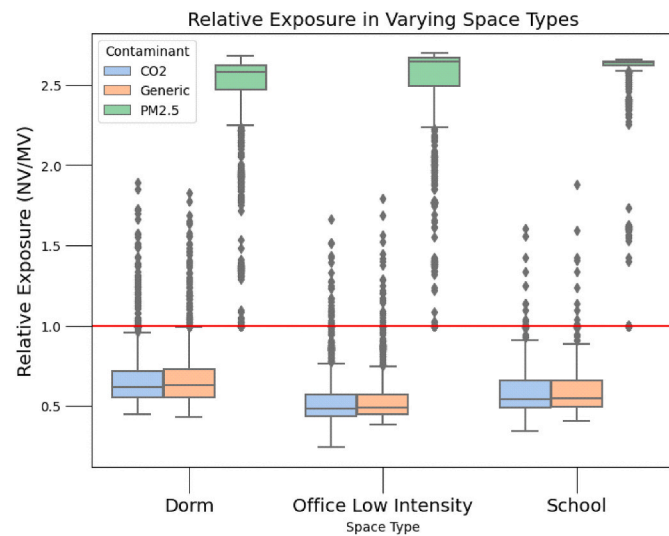


Fig. 7. Sensitivity to space type.

openings prescribed, the exposure varied almost solely with outdoor concentration, amount of MV usage, and most importantly, filter efficiency. During times when NV was in use, room concentrations quickly reached levels near the outdoor concentrations and thus exposure was effectively only a function of outdoor concentration, and ventilation mode. Again, we note a large discrepancy in exposure across climates, owing to the disparities in outdoor air quality, and amount of time suitable for natural ventilation.

Across the simulations, there was an average of 2.1–2.5 times the fine particle concentration during occupied hours, when utilizing the ASHRAE 62.1–19 NV openings instead of MV with prescribed using the VRP and the minimum required MERV-8 filter. If a more effective filter were to be used, the difference between NV and MV would increase. For example, we calculated 7.8–10.4 the annual average fine particle concentration when comparing the NV openings to the MV case using a

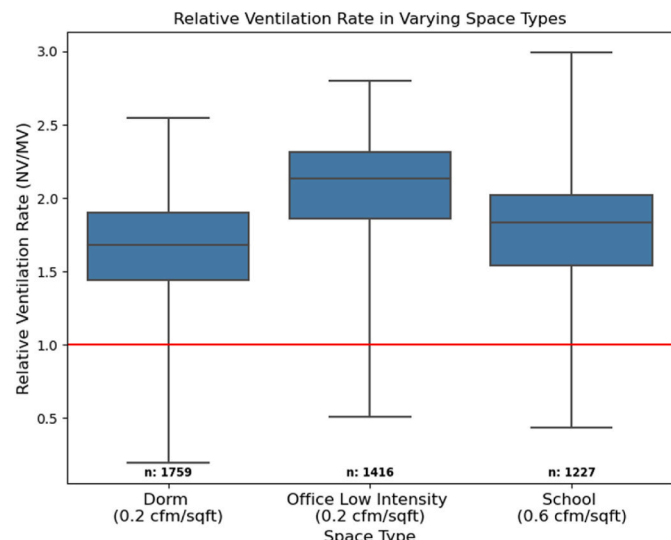


Fig. 8. Sensitivity to Space Type. (n refers to the number of occupied hours suitable for natural ventilation).

MERV-13 filter. To compare further, Table 5 summarizes the distribution of annual average relative concentration of fine particles observed in simulations across all locations, occupant densities, and filters. Variation among the average relative exposure in the NV cases can be attributed to the differences in number of hours available for NV across locations and the local outdoor fine particle concentration and occupancy during those available hours. Relative concentration did not vary greatly based on assumed occupant density or geometry.

3.5. Sensitivity to input assumptions

In this section additional models were formulated for a representative climate, San-Francisco, to determine the sensitive to various

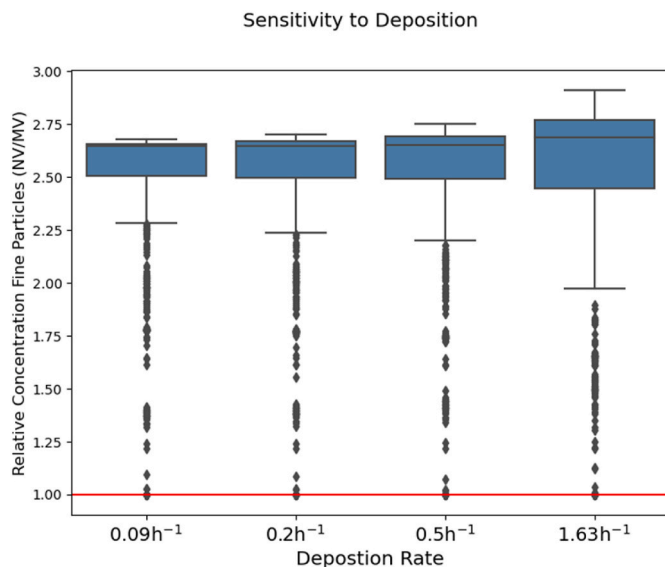


Fig. 9. Sensitivity to deposition.

parameters. Two main variables were tested: particle space type, which is the determining factor in most inputs such as schedules, internal loads, and occupancy, and deposition rate.

3.5.1. Space type

Fig. 7 shows the relative concentrations of the three pollutants modeled, with a red line denoting the concentration provided by the VRP. Only small variations exist between space types in terms of relative concentration of all three pollutants, however the office space had notably lower relative concentrations of CO₂ and the generic contaminant. The lower relative concentrations coincide with the findings presented in Fig. 8. The office space had higher natural ventilation rates relative to the VRP because of the corresponding occupancy, loads, and schedules associated with the space.

3.5.2. Sensitivity to particle deposition

We tried various inputs used in previous studies for deposition rate in the San Francisco climate with a MERV 8 filter as seen in Fig. 9. Relative concentration of fine particles was not sensitive to input particle deposition rate, although the extreme rate of 1.63 h⁻¹ did yield a median outside of the inter quartiles of the smaller values. This indicates that transport into the building via natural ventilation dominates the mass balance for fine particles relative to deposition. Fig. 9 also reinforces the assessment that natural ventilation introduces particles at a much higher rate than the VRP, while asserting that the finding is not sensitive to model inputs for particle loss due to deposition.

3.6. Limitations

The modeling methods outlined in this research are meant to give an approximation of the resulting behavior of naturally ventilated buildings. However, our approach has the following assumptions which will lead to some discrepancy between real concentrations and those reported:

- Uncertainty in particle sources, sinks, or deposition
- No external gaseous pollutant sources

The exclusion of external gaseous pollutant sources for the generic contaminant could potentially cause underestimation of the relative concentration. Recalling, the generic pollutant is meant to capture gaseous contaminants such as VOCs emitted by the building; an outdoor

source of these pollutants would likely result in outdoor concentrations orders of magnitude less than the indoor concentration. However, some gaseous pollutants generated primarily outside, such as NO₂, were not considered.

Additional sources of uncertainty in the simulations may include weather files employed and disparity between local fine particle concentrations and those reported in the reference year at EPA monitoring stations, used for the simulation campaign. We also modeled a single-story building. Pollutant and wind speed boundary conditions at openings of taller buildings will vary. Pollutant concentrations in this case were measured at EPA monitoring stations at heights approximately the same as openings of a one-story building and thus will be conservative at higher elevations. However, wind speeds will increase at higher elevations and thus NV rates are expected to increase as well.

Lastly, in this study, natural ventilation is being considered only as an air quality control strategy because we are investigating IAQ impacts of meeting Standard 62.1-19, "Ventilation for Acceptable Indoor Air Quality." NV openings are often designed to meet thermal comfort goals and bring in ventilation rates much greater than those in this simulation. In cases where the ventilation rates are much higher than the VRP rates, it may be difficult to effectively address the introduction of particles from NV.

4. Discussion

4.1. Current standard specifies effective NV rates greater than the MV standard

Figs. 3 and 4 point to effective ventilation rates in NV spaces designed with 62.1-2019 that are multiples of those in the VRP procedure. While, as mentioned previously, the rationale for the new prescriptions of opening sizes in 62.1 is not well understood, it is generally acknowledged that NV designs involve introducing much more air than is required for air quality control, as a means of displacing thermal loads. However, as a minimum prescribed in an air quality standard, Fig. 3 points to a large disparity between the MV and NV procedures given in 62.1 with regards to how much air they effectively prescribe to be brought into buildings. Bringing in more air than is needed has some negative consequences as described below.

4.1.1. Comparison to previous version of Standard 62.1

The older version of the Standard provided ventilation rates that did not consider geometry, only specifying opening sizes equal to 4% of floor area for any geometry or climate. In order to quantify the impact of the changes to the standard, Table 6 summarizes the ventilation intensity (V_{bz}/A_z) in 62.1-19 that provides similar ventilation rates to previous versions of the code. In other words, Table 6 shows the inherent assumption for ventilation intensity in the pre-2019 version of the Standard. For geometries with two openings, (D and E), the previous standard provided amounts of ventilation air only appropriate for higher occupant densities. The other single opening geometries would have provided enough ventilation for low density spaces as compared to the updated version of the standard.

4.2. Climate sensitivity

Figs. 3 and 6 show a clear disparity in resulting ventilation rates among some climates. This is to be expected to some degree because of the variation in wind and outdoor temperature (and thus stack driven flow) across climates. However, it points to an area of improvement in the standard, as climate seems to be at least as important of a variable as geometry or occupant density in determining acceptability of ventilation strategy. It should be noted that there is precedent for climate-dependent specification of ventilation rates, such as the concept of the "weather and shielding factor" in ASHRAE Standard 62.2 [64].

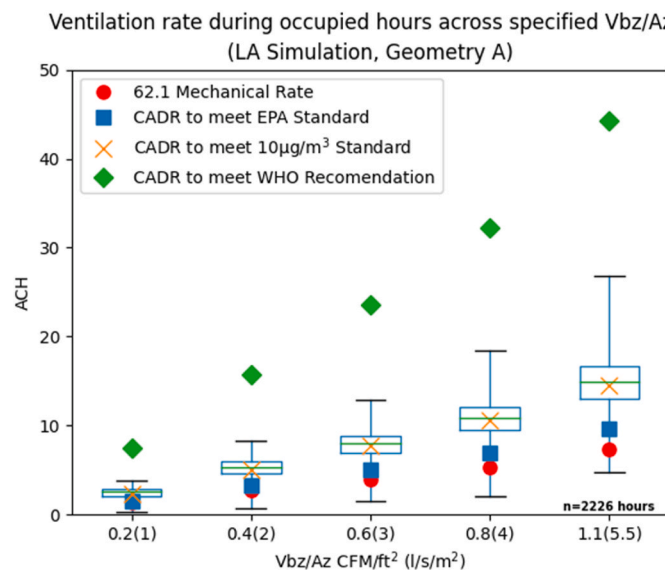


Fig. 10. LA Natural Ventilation rates and corresponding CADR to comply with various standards. (n refers to the number of occupied hours suitable for natural ventilation).

4.3. Implications of comparison of resulting concentrations between MV and NV

Both the results of the generic indoor-generated contaminant simulation and the corresponding fine particle analysis results call into question the approach of specifying opening sizes only for NV, in an air quality standard. Despite more air being introduced than for the MV case, the resulting air quality is substantially degraded because of the drastically elevated indoor particle concentrations, due to the lack of filtration. This is the mechanism shown in previous work to result in increased morbidity and mortality if substantial portions of the building stock are converted to NV [27]. It also undermines the rationale for offering green building designation, in part, for buildings employing NV. At least one popular green building standard confers points for improved indoor environmental quality to buildings employing NV, presumably because NV buildings typically have greater outdoor air supply rates. However, the introduction of fine particles from outside, with their outsized effects on human health, negates any marginal improvement to concentrations of VOCs and odors generated indoors, as has been pointed out previously.

4.4. Consequences for particle exposure mitigation strategy

There is one design strategy that could mitigate the issue of increased particle exposure in NV buildings, but it is less feasible when more air is introduced than is needed, which seems to be the case in NV buildings designed with 62.1–2019 as shown in Section 3.2 of this work. If the goal of NV is only air quality control (sometimes done in conjunction with parallel sensible device such as chilled beams or radiant panels) stand-alone filtration within the spaces with portable or fixed HEPA filters can conceivably reduce particle concentrations to or below those resulting in the MV cases, and likely for much less energy consumption than a full central conditioning system. This strategy has been explored in the literature previously [65]. However, as shown, Standard 62.1–2019 effectively specifies greater NV ventilation rates than are needed in all climates, making it more difficult to filter these particles, while at the same time not requiring any filtration, resulting in air quality substantially worse than the MV case.

To further explore the idea of combining recirculating filtration with natural ventilation, for each location the annual average of the simulated indoor particle concentrations was calculated and compared to the

U.S. National Ambient Air Quality Standard (NAAQS-2020) of $12 \mu\text{g}/\text{m}^3$ annual limit, and the WHO recommendation of a $5 \mu\text{g}/\text{m}^3$ average annual limit [66]. A $10 \mu\text{g}/\text{m}^3$ annual limit was also considered for the possibility of the development of a more conservative national standard. Using the annual average natural ventilation rate for each location and the assumed deposition rate, we calculated a clean air delivery rate (CADR) required to maintain the respective fine particle standard in each location.

Figs. 10 and 11 display the natural ventilation rate for the simulations in air changes per hour (ACH) in box plots as a function of the ventilation intensity (and thus occupant density), as calculated in Equation (1). The red “Mechanical Rate” dots show the VRP ventilation rate prescribed with Equation (1), again displaying the disparity in the amount of ventilation air brought in using the NVP instead of the VRP. Lastly, the other markers show the clean air delivery rate, (CADR) required to uphold the respective standards specified in the legend calculated as described above.

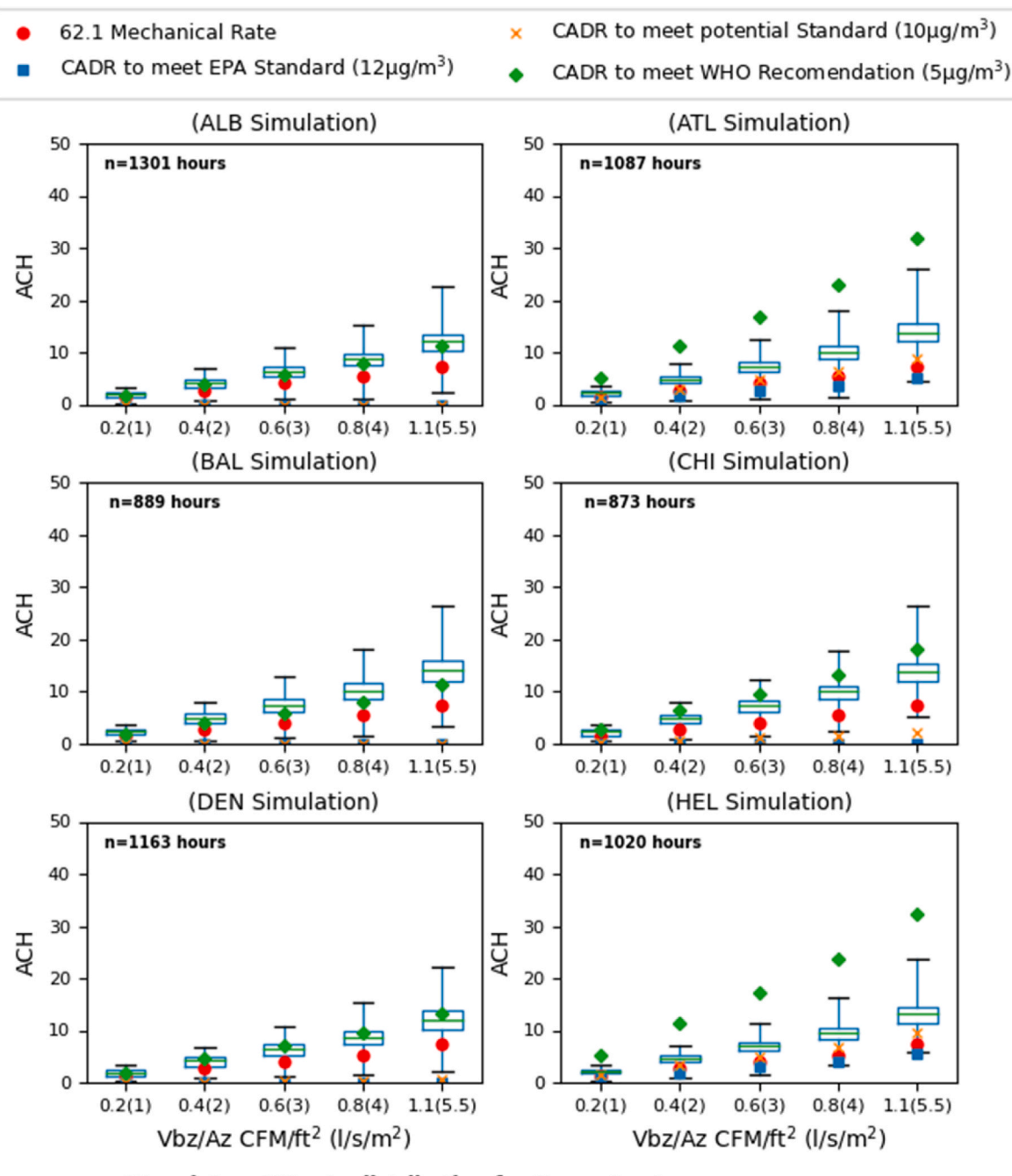
If recirculating filtration were to be added to ensure the NAAQS-2020 limits were met, Fig. 7 shows, the CADR of the recirculating filtration system needed for each occupant density in the Los Angeles simulation. Referencing Fig. 10, it is necessary to clean more air than would be provided by the specified VRP ventilation rate to uphold the current EPA standard in Los Angeles. Note that Los Angeles is currently an EPA non-attainment zone for particles, which highlights the importance of considering local air quality while designing buildings for natural ventilation. It also serves an “upper bound” and points to the fact that achievable CADR values could be provided to meet current EPA thresholds, if the effective NV rates were to decrease to meet the MV rates.

Fig. 11a and b show the results of the CADR analysis for the remaining 12 locations simulated, none of which are currently designated as non-attainment by the EPA. For the years analyzed for average fine particle concentration, eight locations would have needed a CADR of zero, meaning no additional filtration at the natural ventilation rates simulated to meet the current EPA $12 \mu\text{g}/\text{m}^3$ standard. Four locations would not need additional filtration to meet the potential $10 \mu\text{g}/\text{m}^3$ standard. Across all locations, the WHO air quality guidelines could not be met by using NV without filtration. Additionally, in many cases, providing enough filtration to meet the WHO air quality guidelines may not be feasible in the years investigated because of the low concentration limits.

5. Conclusion and limitations

The work described herein led to a few overarching conclusions that may inform future development of ventilation and air quality standards or design of buildings based on them. In general:

- The prescriptive NV Procedure in Standard 62.1 is expected to result in greater quantities of air being introduced into spaces than its MV counterpart. We suggest amending the procedure to more closely reflect the consensus rates contained in the VRP.
- For most hours of the year, this results in somewhat reduced concentrations of pollutants generated indoors, including those generated by occupants and those generated by the building itself. The building-generated and occupant-generated pollutants behaved similarly.
- This improvement in air quality is negated by the introduction of more fine particles from outdoors in all locations analyzed. With current minimum prescriptions of MERV-8 filters this results in a significant but relatively small increase in fine particle concentrations in NV buildings over their MV counterparts. However, compared to mechanical ventilation with MERV-13 filters, the disparity between the two cases is magnified greatly. We understand this latter situation is present in many commercial buildings and may become standardized in the future. We believe this highlights the



*Boxplots = NV rate distribution for Geometry A

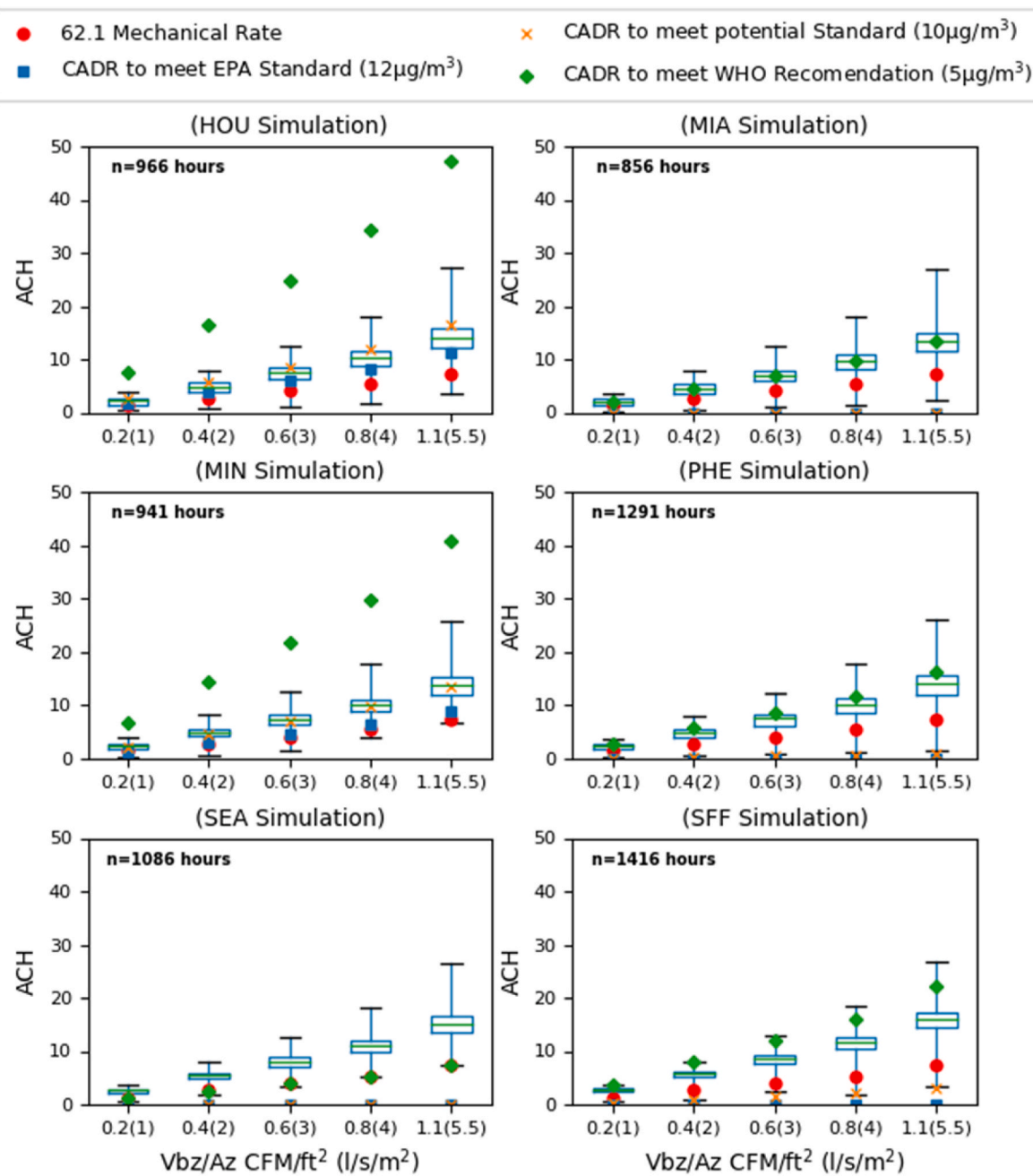
Fig. 11a. Natural Ventilation rates and corresponding CADR to comply with various standards.

need for addressing the increased particle penetration in NV buildings. Suggestions for doing so are below.

- Climate and location play an outsized role in determining both the amount of ventilation air and the resulting IAQ that results from application of the Standard 62.1 NVP Prescriptions, despite not being accounted for in the current prescriptions. We suggest including climate-specific prescriptions, as is done in other locations in ASHRAE ventilation standards.
- Some disparity was discovered among the rates resulting from different geometries of openings, although this was less than that resulting from different climates. Especially in the case of two openings, geometry requirements can be tweaked to come more in line with the VRP.

- In all but the least occupant densities, the changes in the 2019 standard result in substantially increased amount of filtration required to maintain NAAQS-2020-specified limits on fine particle concentrations, over previous versions of the standards.

Despite the shortcomings outlined above, we show that meeting current NAAQS-2020 thresholds indoors is likely feasible in NV spaces in most locations, with properly prescribed geometries and properly sized filtration. This involves specifying parallel filtration and reducing effective NV rates to meet MV counterparts. Similar measures are already being considered in response to increased wildfire incidence and airborne infectious disease concerns and will substantially improve air quality in NV buildings.



*Boxplots = NV rate distribution for Geometry A

Fig. 11b. Natural Ventilation rates and corresponding CADR to comply with various standards

CRediT authorship contribution statement

Troye Sas-Wright: Writing – original draft, Software, Investigation, Formal analysis. **Jordan D. Clark:** Writing – review & editing, Supervision, Project administration, Methodology, Conceptualization.

Declaration of competing interest

The authors declare that they have no known competing financial interests or personal relationships that could have appeared to influence the work reported in this paper.

Acknowledgement

The authors would like to thank the following programs for supporting this work through scholarships and fellowships:

- The Ohio State University, College of Engineering Undergraduate Honors Research Scholarship.
- The Ohio State University, Department of Civil, Environmental, and Geodetic Engineering Summer Undergraduate Research Fellowship (SURF).
- The Ohio State University Graduate Enrichment Fellowship Program.

In addition, the authors would like to thank Mr. Stuart Dols at the National Institute of Standards and Technology for his guidance in using the simulation framework.

Appendix

Table A-1
Opening Geometry Dimensions

A_o/V_{lbz} cfm/ft ² ([L/s]/m ²)	Geometry	Description	Opening 1 area ft ² (m ²)	Opening 2 area ft ² (m ²)
0.2 (1)	2:01	Tall	4.5 (0.42)	n/a
0.4 (2)	2:01	Tall	7.92 (0.74)	n/a
0.6 (3)	2:01	Tall	10.8 (1.00)	n/a
0.8 (4)	2:01	Tall	13.68 (1.27)	n/a
1.1 (5.5)	2:01	Tall	17.64 (1.64)	n/a
0.2 (1)	1:01	square	5.22 (0.48)	n/a
0.4 (2)	1:01	square	9 (0.84)	n/a
0.6 (3)	1:01	square	12.42 (1.15)	n/a
0.8 (4)	1:01	square	15.66 (1.45)	n/a
1.1 (5.5)	1:01	square	20.16 (1.87)	n/a
0.2 (1)	1:10	Thin, long	20.16 (1.87)	n/a
0.4 (2)	1:10	Thin, long	34.78 (3.23)	n/a
0.6 (3)	1:10	Thin, long	47.88 (4.45)	n/a
0.8 (4)	1:10	Thin, long	60.48 (5.62)	n/a
1.1 (5.5)	1:10	Thin, long	78.12 (7.26)	n/a
0.2 (1)	1:02	Vertically spaced, unequal sizes	1.2 (0.11)	2.4 (0.22)
0.4 (2)	1:02	Vertically spaced, unequal sizes	2.4 (0.22)	4.8 (0.45)
0.6 (3)	1:02	Vertically spaced, unequal sizes	3.6 (0.33)	7.2 (0.67)
0.8 (4)	1:02	Vertically spaced, unequal sizes	4.8 (0.45)	9.6 (0.89)
1.1 (5.5)	1:02	Vertically spaced, unequal sizes	6.6 (0.61)	13.2 (1.23)
0.2 (1)	1:02	Vertically spaced, equal sizes	1.17 (0.11)	1.17 (0.11)
0.4 (2)	1:02	Vertically spaced, equal sizes	2.34 (0.22)	2.34 (0.22)
0.6 (3)	1:02	Vertically spaced, equal sizes	3.51 (0.33)	3.51 (0.33)
0.8 (4)	1:02	Vertically spaced, equal sizes	4.68 (0.43)	4.68 (0.43)
1.1 (5.5)	1:02	Vertically spaced, equal sizes	6.39 (0.59)	6.39 (0.59)

Table A-2

Roof U-Values [33]

Table 19 Roof U-Values (Btu/h·ft²·°F) by Reference Building Vintage

Location	90.1–2004 Climate Zone	90.1–1989 Table	Pre-1980	Post-1980	New Construction Insulation Above Deck	New Construction Attic
Miami, FL	1A	8A-15	0.100	0.074	0.063	0.034
Houston, TX	2A	8A-10	0.100	0.066	0.063	0.034
Phoenix, AZ	2B	8A-18	0.100	0.046	0.063	0.034
Atlanta, GA	3A	8A-8	0.100	0.072	0.063	0.034
Los Angeles, CA	3B-CA	8A-6	0.100	0.100	0.063	0.034
Las Vegas, NV	3B-other	8A-14	0.100	0.048	0.063	0.034
San Francisco, CA	3C	8A-5	0.100	0.088	0.063	0.034
Baltimore, MD	4A	8A-25	0.086	0.058	0.063	0.034
Albuquerque, NM	4B	8A-23	0.089	0.059	0.063	0.034
Seattle, WA	4C	8A-19	0.085	0.064	0.063	0.034
Chicago, IL	5A	8A-26	0.072	0.053	0.063	0.034
Denver, CO	5B	8A-28	0.076	0.051	0.063	0.034
Minneapolis, MN	6A	8A-33	0.060	0.045	0.063	0.027
Helena, MT	6B	8A-32	0.060	0.049	0.063	0.027
Duluth, MN	7	8A-36	0.060	0.040	0.063	0.027
Fairbanks, AK	8	8A-38	0.060	0.031	0.048	0.027

Table A-3

Wall U-Values [33]

Table 20 Steel Frame Wall U-Values (Btu/h·ft²·°F) by Reference Building Vintage

Location	90.1–2004 Climate Zone	90.1–1989 Table	Pre-1980		Post-1980		New Construction	
			Btu/h·ft ² ·°F	W/m ² ·K	Btu/h·ft ² ·°F	W/m ² ·K	Btu/h·ft ² ·°F	W/m ² ·K
Miami, FL	1A	8A-15	0.230	1.306	1.000	5.678	0.124	0.704
Houston, TX	2A	8A-10	0.230	1.306	0.150	0.852	0.124	0.704
Phoenix, AZ	2B	8A-18	0.230	1.306	0.240	1.363	0.124	0.704
Atlanta, GA	3A	8A-8	0.225	1.278	0.130	0.738	0.124	0.704
Los Angeles, CA	3B-CA	8A-6	0.230	1.306	0.220	1.249	0.124	0.704
Las Vegas NV	3B-other	8A-14	0.230	1.306	0.160	0.909	0.124	0.704

(continued on next page)

Table A-3 (continued)

Location	90.1–2004 Climate Zone	90.1–1989 Table	Pre-1980		Post-1980		New Construction	
			Btu/h·ft ² ·°F	W/m ² ·K	Btu/h·ft ² ·°F	W/m ² ·K	Btu/h·ft ² ·°F	W/m ² ·K
San Francisco, CA	3C	8A-5	0.224	1.272	0.130	0.738	0.124	0.704
Baltimore, MD	4A	8A-25	0.178	1.011	0.089	0.505	0.124	0.704
Albuquerque, NM	4B	8A-23	0.184	1.045	0.100	0.568	0.124	0.704
Seattle, WA	4C	8A-19	0.175	0.994	0.092	0.522	0.124	0.704
Chicago, IL	5A	8A-26	0.156	0.886	0.082	0.466	0.084	0.477
Denver, CO	5B	8A-28	0.161	0.914	0.082	0.466	0.084	0.477
Minneapolis, MN	6A	8A-33	0.145	0.823	0.065	0.369	0.084	0.477
Helena, MT	6B	8A-32	0.145	0.823	0.072	0.409	0.084	0.477
Duluth, MN	7	8A-36	0.136	0.772	0.058	0.329	0.064	0.363
Fairbanks, AK	8	8A-38	0.125	0.710	0.045	0.256	0.064	0.363

Table A-4

Relative ventilation rate grouped by location.

Location	mean	std	min	25%	50%	75%	max
ALB	1.69	0.23	1.41	1.53	1.59	1.77	2.18
ATL	1.97	0.26	1.65	1.78	1.86	2.06	2.53
BAL	1.97	0.26	1.65	1.78	1.86	2.05	2.51
CHI	1.94	0.26	1.61	1.75	1.82	2.02	2.48
DEN	1.71	0.23	1.42	1.54	1.61	1.79	2.19
HEL	1.90	0.26	1.61	1.73	1.82	1.97	2.41
HOU	1.97	0.26	1.62	1.79	1.86	2.07	2.53
LAA	2.13	0.28	1.82	1.95	2.05	2.21	2.70
MIA	1.85	0.26	1.52	1.68	1.76	1.95	2.40
MIN	1.96	0.26	1.64	1.77	1.85	2.04	2.50
PHE	1.97	0.26	1.66	1.78	1.88	2.04	2.51
SEA	2.19	0.29	1.90	2.00	2.09	2.24	2.75
SFF	2.28	0.30	1.99	2.07	2.18	2.33	2.85

Table A-5

Relative ventilation rate grouped by occupancy density.

OccDensity Cfm/sqft (l/s/m ²)	mean	std	min	25%	50%	75%	max
0.2(1)	1.86	0.31	1.41	1.63	1.78	2.00	2.79
0.4(2)	1.94	0.30	1.49	1.74	1.86	2.08	2.82
0.6(3)	1.98	0.30	1.52	1.77	1.92	2.11	2.82
0.8(4)	2.02	0.30	1.57	1.82	1.95	2.16	2.85
1.1(5.5)	2.03	0.29	1.59	1.83	1.97	2.18	2.84

Table A-6

Relative ventilation rate grouped by geometry.

Geometry	mean	std	min	25%	50%	75%	max
A	1.77	0.16	1.41	1.65	1.76	1.85	2.08
B	1.76	0.16	1.41	1.66	1.75	1.84	2.08
C	1.88	0.16	1.51	1.77	1.88	1.96	2.21
D	2.43	0.21	1.97	2.31	2.43	2.53	2.85
E	1.98	0.18	1.59	1.86	1.97	2.06	2.34

Table A-7

Space Type Load and Source Strength Assumptions

Space Type	Lighting load (w/m ²)	Equipment Load (w/m ²)	CO ₂ Breathing Rate (L/s)
Office	10.76	10.76	0.0051
School >9 Year olds	15.06	15	0.0063
Bedroom	3.88	5.38	0.0036

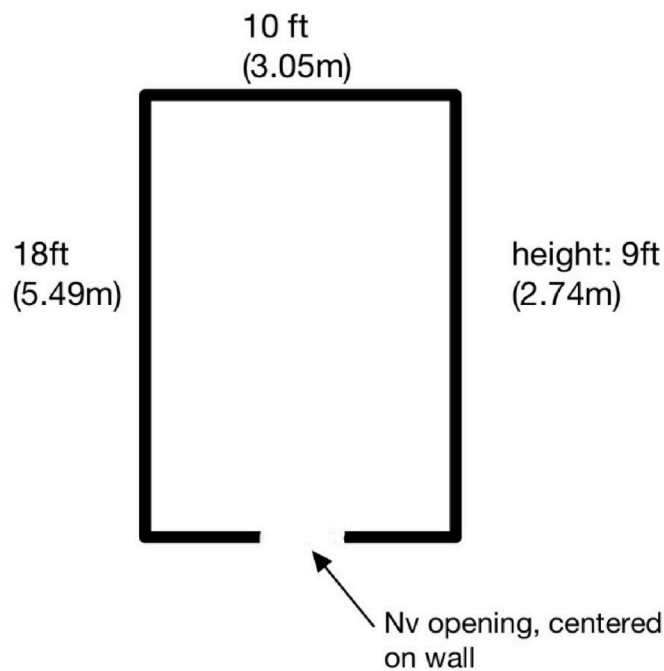


Fig. A1. Zone Geometry

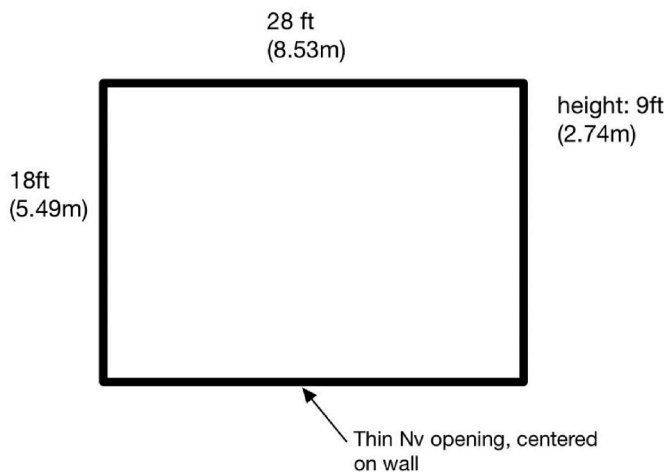


Fig. A2. Zone Geometry for 1:10 Opening Geometry

References

- [1] J. Chen, G. Augenbroe, Z. Zeng, X. Song, Regional difference and related cooling electricity savings of air pollutant affected natural ventilation in commercial buildings across the US, *Build. Environ.* 172 (Apr. 2020), 106700, <https://doi.org/10.1016/J.BUILDENV.2020.106700>.
- [2] Linden, P.; Banks, D.; Daish, N.; Fountain, M.; Gross, G.; Honnepkeri, A., et al. (2016). Natural Ventilation for Energy Savings in California Commercial Buildings. UC Berkeley: Center for the Built Environment. Retrieved from <https://escholarship.org/uc/item/4cd38657K>. Adams, et al., Natural ventilation for energy savings in California commercial buildings, Final report to CEC. November. (2014).
- [3] T. Ben-David, M.S. Waring, Impact of natural versus mechanical ventilation on simulated indoor air quality and energy consumption in offices in fourteen U.S. cities, *Build. Environ.* 104 (Aug. 2016) 320–336, <https://doi.org/10.1016/J.BUILDENV.2016.05.007>.
- [4] R. De Dear, G.S. Brager, *Developing an Adaptive Model of Thermal Comfort and Preference*, 1998.
- [5] H.Y. Zhong, et al., Single-sided natural ventilation in buildings: a critical literature review, *Build. Environ.* 212 (Mar. 2022), <https://doi.org/10.1016/J.BUILDENV.2022.108797>.
- [6] G. Carrilho da Graça, P. Linden, Ten questions about natural ventilation of non-domestic buildings, *Build. Environ.* 107 (Oct. 2016) 263–273, <https://doi.org/10.1016/J.BUILDENV.2016.08.007>.
- [7] L.J. Lo, A. Novoselac, Cross ventilation with small openings: measurements in a multi-zone test building, *Build. Environ.* 57 (Nov. 2012) 377–386, <https://doi.org/10.1016/J.BUILDENV.2012.06.009>.
- [8] L. James Lo, D. Banks, A. Novoselac, Combined wind tunnel and CFD analysis for indoor airflow prediction of wind-driven cross ventilation, *Build. Environ.* 60 (Feb. 2013) 12–23, <https://doi.org/10.1016/J.BUILDENV.2012.10.022>.
- [9] J. Cheng, D. Qi, A. Katal, L. (Leon), Wang, T. Stathopoulos, Evaluating wind-driven natural ventilation potential for early building design, *J. Wind Eng. Ind. Aerod.* 182 (Nov. 2018) 160–169, <https://doi.org/10.1016/J.JWEIA.2018.09.017>.
- [10] Y. Arinami, S. ichi Akabayashi, Y. Tominaga, J. Sakaguchi, Performance evaluation of single-sided natural ventilation for generic building using large-eddy simulations: effect of guide vanes and adjacent obstacles, *Build. Environ.* 154 (May 2019) 68–80, <https://doi.org/10.1016/J.BUILDENV.2019.01.021>.
- [11] D. Etheridge, A perspective on fifty years of natural ventilation research, *Build. Environ.* 91 (Sep. 2015) 51–60, <https://doi.org/10.1016/J.BUILDENV.2015.02.033>.
- [12] J. Wang, T. Zhang, S. Wang, F. Battaglia, Gaseous pollutant transmission through windows between vertical floors in a multistory building with natural ventilation,

Energy Build. 153 (Oct. 2017) 325–340, <https://doi.org/10.1016/J.ENBUILD.2017.08.025>.

[13] Y. Jiang, D. Alexander, H. Jenkins, R. Arthur, Q. Chen, Natural ventilation in buildings: measurement in a wind tunnel and numerical simulation with large-eddy simulation, *J. Wind Eng. Ind. Aerod.* 91 (3) (Feb. 2003) 331–353, [https://doi.org/10.1016/S0167-6105\(02\)00380-X](https://doi.org/10.1016/S0167-6105(02)00380-X).

[14] A.D. Stavridou, P.E. Prinos, Natural ventilation of buildings due to buoyancy assisted by wind: investigating cross ventilation with computational and laboratory simulation, *Build. Environ.* 66 (Aug. 2013) 104–119, <https://doi.org/10.1016/J.BUILDENV.2013.04.011>.

[15] Z. Jiang, et al., Validity of Orifice equation and impact of building parameters on wind-induced natural ventilation rates with minute mean wind pressure difference, *Build. Environ.* 219 (Jul. 2022), 109248, <https://doi.org/10.1016/J.BUILDENV.2022.109248>.

[16] D.P. Albuquerque, P.D. O'Sullivan, G.C. da Graça, Effect of window geometry on wind driven single sided ventilation through one opening, *Energy Build.* 245 (Aug. 2021), <https://doi.org/10.1016/J.ENBUILD.2021.111060>.

[17] W.S. Dols, S.J. Emmerich, B.J. Polidoro, Coupling the multizone airflow and contaminant transport software CONTAM with EnergyPlus using co-simulation, *Build. Simulat.* 9 (4) (Aug. 2016) 469–479, <https://doi.org/10.1007/S12273-016-0279-2>.

[18] W.S. Dols, C.W. Milano, L. Ng, S.J. Emmerich, J. Teo, On the benefits of whole-building IAQ, ventilation, infiltration, and energy analysis using Co-simulation between CONTAM and EnergyPlus, in: *Journal of Physics: Conference Series*, IOP Publishing, 2021, 012183.

[19] B.D. Less, S.M. Dutton, I.S. Walker, M.H. Sherman, J.D. Clark, Energy savings with outdoor temperature-based smart ventilation control strategies in advanced California homes, *Energy Build.* 194 (Jul. 2019) 317–327, <https://doi.org/10.1016/J.ENBUILD.2019.04.028>.

[20] I. Walker, M. Young, B. Less, S. Dutton, M. Sherman, J. Clark, Assessment of Peak Power Demand Reduction Available via Modulation of Building Ventilation Systems, 2022.

[21] J.D. Clark, B.D. Less, S.M. Dutton, I.S. Walker, M.H. Sherman, Efficacy of occupancy-based smart ventilation control strategies in energy-efficient homes in the United States, *Build. Environ.* 156 (Jun. 2019) 253–267, <https://doi.org/10.1016/J.BUILDENV.2019.03.002>.

[22] ASHRAE, *ANSI/ASHRAE Standard 62, 2019*, pp. 1–2019.

[23] T. Ruan, D. Rim, Indoor air pollution in office buildings in mega-cities: effects of filtration efficiency and outdoor air ventilation rates, *Sustain. Cities Soc.* 49 (Aug. 2019), <https://doi.org/10.1016/J.JSCS.2019.101609>.

[24] N.R. Martins, G. Carrilho da Graça, Impact of outdoor PM2.5 on natural ventilation usability in California's nondomestic buildings, *Appl. Energy* 189 (2017) 711–724, <https://doi.org/10.1016/J.APENERGY.2016.12.103>.

[25] L. Stabile, M. Dell'Isola, A. Russi, A. Massimo, G. Buonanno, The effect of natural ventilation strategy on indoor air quality in schools, *Sci. Total Environ.* 595 (Oct. 2017) 894–902, <https://doi.org/10.1016/J.SCITOTENV.2017.03.048>.

[26] N.R. Martins, G. Carrilho da Graça, Simulation of the effect of fine particle pollution on the potential for natural ventilation of non-domestic buildings in European cities, *Build. Environ.* 115 (Apr. 2017) 236–250, <https://doi.org/10.1016/J.BUILDENV.2017.01.030>.

[27] S.M. Dutton, D. Banks, S.L. Brunswick, W.J. Fisk, Health and economic implications of natural ventilation in California offices, *Build. Environ.* 67 (Sep. 2013) 34–45, <https://doi.org/10.1016/J.BUILDENV.2013.05.002>.

[28] A. Chen, E.T. Gall, V.W.C. Chang, Indoor and outdoor particulate matter in primary school classrooms with fan-assisted natural ventilation in Singapore, *Environ. Sci. Pollut. Control Ser.* 23 (17) (Sep. 2016) 17613–17624, <https://doi.org/10.1007/S11356-016-6826-7/METRICS>.

[29] World Health Organization, Ambient (Outdoor) Air Pollution, World Health Organization Newsroom, 2021. Sep. 22, [https://www.who.int/news-room/fact-sheets/detail/ambient-\(outdoor\)-air-quality-and-health](https://www.who.int/news-room/fact-sheets/detail/ambient-(outdoor)-air-quality-and-health). (Accessed 4 June 2023).

[30] J. Chen, G.S. Brager, G. Augenbroe, X. Song, Impact of outdoor air quality on the natural ventilation usage of commercial buildings in the US, *Appl. Energy* 235 (Feb. 2019) 673–684, <https://doi.org/10.1016/J.APENERGY.2018.11.020>.

[31] A.K. Persily, Field measurement of ventilation rates, *Indoor Air* 2014 26 (1) (Feb. 2016) 97–111, <https://doi.org/10.1111/ina.12193>.

[32] E. McConahey, The Feasibility of Natural Ventilation.” Nov. 07, 2019 [Online]. Available: https://svjashrae.starchapter.com/images/downloads/Natural_Ventilation.pdf.

[33] M. Deru, et al., U.S. Department of Energy Commercial Reference Building Models of the National Building Stock, *Publications (E)*, Feb., 2011. Accessed: Jun. 06, 2023. [Online]. Available: https://digitalscholarship.unlv.edu/renew_pubs/44.

[34] W. Dols, B. Polidoro, CONTAM User Guide and Program Documentation, 2015, <https://doi.org/10.6028/NIST.TN.1887r1>. Gaithersburg, MD, version 3.2.

[35] DOE, EnergyPlus Documentation [Online]. Available:, US Department of Energy, 2010 <https://energyplus.net/documentation>.

[36] S. Wilcox, W. Marion, Users Manual for TMY3 Data Sets, 2008. Accessed: Jun. 04, 2023. [Online]. Available: https://www.doe2.com/Download/Weather/TMY3/Users_Manual_for_TMY3_Data_Sets.pdf.

[37] S. Emmerich, B. Polidoro, J.A.-E. Buildings, undefined, Impact of adaptive thermal comfort on climatic suitability of natural ventilation in office buildings, Elsevier 43 (9) (2011) 2101–2107, <https://doi.org/10.1016/j.enbuild.2011.04.016>. Sep. 2011.

[38] L. Morawska, et al., Airborne particles in indoor environment of homes, schools, offices and aged care facilities: the main routes of exposure, *Environ. Int.* 108 (Nov. 2017) 75–83, <https://doi.org/10.1016/J.ENVINT.2017.07.025>.

[39] M. Zaatari, A. Novoselac, J. Siegel, The relationship between filter pressure drop, indoor air quality, and energy consumption in rooftop HVAC units, *Build. Environ.* 73 (Mar. 2014) 151–161, <https://doi.org/10.1016/J.BUILDENV.2013.12.010>.

[40] T. Ben-David, M.W.-B. Environment, undefined, Impact of Natural versus Mechanical Ventilation on Simulated Indoor Air Quality and Energy Consumption in Offices in Fourteen US Cities, Elsevier, 2016. Accessed: Jun. 04, 2023. [Online]. Available: <https://www.sciencedirect.com/science/article/pii/S0360132316301597>.

[41] Y. Zhou, G. Yang, S. Xin, Y. Yang, An evaluation model of indoor PM2.5 dynamic characteristics considering human activities, *Energy Build.* 263 (May 2022), 112037, <https://doi.org/10.1016/J.ENBUILD.2022.112037>.

[42] T. Marsik, R. Johnson, HVAC air-quality model and its use to test a PM2.5 control strategy, *Build. Environ.* 43 (11) (Nov. 2008) 1850–1857, <https://doi.org/10.1016/J.BUILDENV.2007.11.001>.

[43] C. Liu, J. Yang, S. Ji, Y. Lu, P. Wu, C. Chen, Influence of natural ventilation rate on indoor PM2.5 deposition, *Build. Environ.* 144 (Oct. 2018) 357–364, <https://doi.org/10.1016/J.BUILDENV.2018.08.039>.

[44] C.M. Long, H.H. Suh, P.J. Catalano, P. Koutrakis, Using time and size-resolved particulate data to quantify indoor penetration and deposition behavior, *Environ. Sci. Technol.* 35 (10) (May 2001) 2089–2099, <https://doi.org/10.1021/ES001477D/ASSET/IMAGES/LARGE/ES001477D00009.JPG>.

[45] L.C. Ng, A. Musser, A.K. Persily, S.J. Emmerich, Indoor air quality analyses of commercial reference buildings, *Build. Environ.* 58 (Dec. 2012) 179–187, <https://doi.org/10.1016/J.BUILDENV.2012.07.008>.

[46] A. Persily and B. J. Polidoro, “Indoor Carbon Dioxide Metric Analysis Tool”, doi: 10.6028/NIST.TN.2213.

[47] M.H. Sherman, I.S. Walker, J.M. Logue, Equivalence in ventilation and indoor air quality, *HVAC R Res.* 18 (4) (Aug. 2012) 760–773, <https://doi.org/10.1080/10789669.2012.667038>.

[48] M.H. Sherman, D.K. Mortensen, I.S. Walker, Derivation of equivalent continuous dilution for cyclic, unsteady driving forces, *Int. J. Heat Mass Tran.* 54 (11–12) (May 2011) 2696–2702, <https://doi.org/10.1016/J.IJHEATMASSTRANSFER.2010.12.018>.

[49] C.J. Weschler, H.C. Shields, D.V. Naik, Indoor Ozone Exposures, *10.1080/08940630.1989.10466650* 39, 2012, pp. 1562–1568, <https://doi.org/10.1080/08940630.1989.10466650>, 12.

[50] E.T. Gall, D. Rim, Mass accretion and ozone reactivity of idealized indoor surfaces in mechanically or naturally ventilated indoor environments, *Build. Environ.* 138 (Jun. 2018) 89–97, <https://doi.org/10.1016/J.BUILDENV.2018.04.030>.

[51] U.S. Environmental Protection Agency, Air data - concentration plot [Online]. Available: <https://www.epa.gov/outdoor-air-quality-data/air-data-concentration-plot>.

[52] W. Dols, CONTAM Parametric Analysis Utilities, 2023 [Online]. Available: <https://www.nist.gov/el/energy-and-environment-division-73200/nist-multizone-modeling/contam-parametric-analysis>.

[53] L. Pinault, et al., Risk estimates of mortality attributed to low concentrations of ambient fine particulate matter in the Canadian community health survey cohort, *Environ. Health 15* (1) (Feb. 2016) 1–15, <https://doi.org/10.1186/S12940-016-0111-6/FIGURES/2>.

[54] Y. Wang, C. Chen, P. Wang, Y. Wan, Z. Chen, L. Zhao, Experimental investigation on indoor/outdoor PM2.5 concentrations of an office building located in guangzhou, *Procedia Eng.* 121 (Jan. 2015) 333–340, <https://doi.org/10.1016/J.PROENG.2015.08.1076>.

[55] I. Rivas, et al., Child exposure to indoor and outdoor air pollutants in schools in Barcelona, Spain, *Environ. Int.* 69 (Aug. 2014) 200–212, <https://doi.org/10.1016/J.JENVINT.2014.04.009>.

[56] M. Elbayoumi, N.A. Ramlı, N.F.F. Md Yusof, Spatial and temporal variations in particulate matter concentrations in twelve schools environment in urban and overpopulated camps landscape, *Build. Environ.* 90 (Aug. 2015) 157–167, <https://doi.org/10.1016/J.BUILDENV.2015.03.036>.

[57] C. M. Ní Riain, D. Mark, M. Davies, R.M. Harrison, M.A. Byrne, Averaging periods for indoor–outdoor ratios of pollution in naturally ventilated non-domestic buildings near a busy road, *Atmos. Environ.* 37 (29) (Sep. 2003) 4121–4132, [https://doi.org/10.1016/S1352-2310\(03\)00509-0](https://doi.org/10.1016/S1352-2310(03)00509-0).

[58] D. Saraga, S. Pateraki, A. Papadopoulos, C. Vasilakos, T. Maggos, Studying the indoor air quality in three non-residential environments of different use: a museum, a printery industry and an office, *Build. Environ.* 46 (11) (Nov. 2011) 2333–2341, <https://doi.org/10.1016/J.BUILDENV.2011.05.013>.

[59] R. Goyal, P. Kumar, Indoor-outdoor concentrations of particulate matter in nine microenvironments of a mix-use commercial building in megacity Delhi, *Air Qual Atmos Health* 6 (4) (Dec. 2013) 747–757, <https://doi.org/10.1007/S11869-013-0212-0/METRICS>.

[60] J. Hu, N. Li, Variation of PM2.5 concentrations in shopping malls in autumn, changsha, *Procedia Eng.* 121 (Jan. 2015) 692–698, <https://doi.org/10.1016/J.J.PROENG.2015.09.006>.

[61] A. Challoner, L. Gill, Indoor/outdoor air pollution relationships in ten commercial buildings: PM2.5 and NO₂, *Build. Environ.* 80 (Oct. 2014) 159–173, <https://doi.org/10.1016/J.BUILDENV.2014.05.032>.

[62] N.Y. Yang Razali, M.T. Latif, D. Dominick, N. Mohamad, F.R. Sulaiman, T. Sritshawirat, Concentration of particulate matter, CO and CO₂ in selected schools in Malaysia, *Build. Environ.* 87 (May 2015) 108–116, <https://doi.org/10.1016/J.BUILDENV.2015.01.015>.

[63] P.V. Dorizas, M.N. Assimakopoulos, C. Helmis, M. Santamouris, An integrated evaluation study of the ventilation rate, the exposure and the indoor air quality in naturally ventilated classrooms in the Mediterranean region during spring, *Sci.*

Total Environ. 502 (Jan. 2015) 557–570, <https://doi.org/10.1016/J.SCITOTENV.2014.09.060>.

[64] ASHRAE, ANSI/ASHRAE Standard 62, 2022, pp. 2–2022.

[65] H. Yin, et al., Field measurement of the impact of natural ventilation and portable air cleaners on indoor air quality in three occupant states, Energy and Built Environment 4 (5) (Oct. 2023) 601–613, <https://doi.org/10.1016/J.ENBENV.2022.05.004>.

[66] World Health Organization, WHO Global Air Quality Guidelines, 2021. <https://apps.who.int/iris/bitstream/handle/10665/345329/9789240034228-eng.pdf>.

[67] Less, Brennan, Dutton, Spencer, Li, Xiwang, Clark, Jordan, Walker, Iain, and Sherman, Max. *Smart Ventilation for Advanced California Homes – Single Zone Technology Task*. United States: N. p., 2019. Web. doi:10.2172/1545146.